A Dumbbell Model for the Structure of Charged, Rodlike Macromolecules in Dilute Solution

Josef Schneider, Walter Hess, and Rudolf Klein*

Fakultät für Physik, Universität Konstanz, D-7750 Konstanz, Federal Republic of Germany.
Received October 4, 1985

ABSTRACT: The static properties of charged, rodlike macroparticles in dilute solution are studied by Monte Carlo simulations. The energy between two rods is supposed to be the sum of the screened Coulomb interactions between two beads on each rod. The pair-distribution function $g(\mathbf{r},\mathbf{u}_1,\mathbf{u}_2)$, its angle average $\bar{g}(r)$, and the intensity of scattered radiation are calculated as a function of the rod length L and are compared with those of charged spheres. With increasing L, the static structure factor is found to exhibit a decreasing main peak which shifts to larger values of the scattering vector.

Structural properties of suspensions of interacting spherical macromolecules have been investigated extensively in recent years. For certain cases like hard-sphere particles and charged spherical particles the predictions for various static properties, which have been obtained by using methods from liquid-state theory, are in excellent agreement with experiment. The basic theoretical quantity is the radial distribution function $g(r)$, from which all thermodynamic properties can be calculated. A very sensitive test for (i) the interaction potential between macroparticles and (ii) for the accuracy of the approximate theories calculating $g(r)$ from the interaction potential, is provided by wave vector dependent properties such as the intensity of scattered radiation $I(k)$, which for spherical scatterers factorizes into a known form factor $F(k)$ and the static structure factor $S(k)$. The latter is given essentially by the Fourier transform of $g(r)$. Calculations of $g(r)$ based on the screened Coulomb potential and using the mean-spherical approximation reproduce the experimental results for $I(k)$ quite well for various systems of charged hard spheres.[1] Also computer simulations are available and are in good agreement with theory and experiment.[2] Qualitatively, $g(r)$ has a rather well-defined main maximum, which defines a shell of nearest neighbors, followed by further secondary extrema, related to further shells and the spaces between them.

In this paper we investigate what happens if each sphere of total charge Q is stretched into a (short) stiff rod of length L, keeping the number concentration of macroparticles constant. The importance of this investigation stems from the increasing interest in systems of charged rodlike particles,[3,4] i.e., in connection with the initial stage of rodlike growth of ionic micelles and scattering experiments on viruses in aqueous solution and on polyelectrolytes.

Since theoretical results for charged rodlike macroparticles are only available for weakly interacting systems[5,6] and are much more complicated to obtain than for spheres, one has to restrict oneself to certain limiting cases. One of them is the limit of rods which are long compared to the mean interaxial distance.[7] Another one is the opposite case, where the length L of each rod is still smaller or at most of the order of the mean distance between their centers of mass. For this case we have performed computer simulations in order to obtain insight into the increasing effects of the anisotropy when L grows. It is obvious that the results of the investigation of this limiting case are not sufficient to describe the details of the experiments mentioned above. The basic theoretical quantity is the angle-dependent pair-distribution function $g(\mathbf{r},\mathbf{u}_1,\mathbf{u}_2)$, where $\mathbf{u}_1$ and $\mathbf{u}_2$ are unit vectors along the rod axes and $\mathbf{r}$ is the vector distance between their centers of mass. Averaging over $\mathbf{u}_1$ and $\mathbf{u}_2$ defines a function $\bar{g}(r)$, which is the object to compare with $g(r)$ for the corresponding case of charged spheres. Results for these functions are presented in the next section.

The scattered intensity $I(k)$ from interacting rods no longer factorizes as for spheres into a product of a form factor and a shape-independent static structure factor, which is simply the Fourier transform of $\bar{g}(r)$. On the basis of the results for $g(\mathbf{r},\mathbf{u}_1,\mathbf{u}_2)$ we show how $I(k)/F(k)$ changes with the length L, keeping Q and the number concentration constant.[8]

Model for the Monte Carlo Simulations

The interaction potential for rods of finite length L has been developed in ref 5; the rods are subdivided into charged segments along the rod axis. The total interaction is then taken as the sum of the screened Coulomb interactions between the segments on different rods. Restricting the concentration to $c < L^{-3}$, we will replace the rods by dumbbells, where each of the beads carries the charge $Q/2$. This simplification keeps the qualitative features of the true potential for high charges and low shielding, which will prevent the rods from coming into contact. This is indicated by the fact that in the simulations no configurations have been found where the center-to-center distance was very small. Therefore, it is unnecessary to include a hard core on the axis for the Q values considered. Representing homogeneously charged rods of length L by dumbbells of length $l = L/3^{1/2}$, the monopole and the quadrupole moments of both objects coincide. Then the interaction between two rods is approximated by

$$U(\mathbf{r},\mathbf{u}_1,\mathbf{u}_2) = \sum_{\alpha,\beta} \frac{(Q/2)^2 e^{-\kappa(r_{\alpha\beta}-2a)}}{4\pi\epsilon\epsilon_0(1+\kappa a)^2 r_{\alpha\beta}} \tag{1}$$

where $r_{\alpha\beta}$ is the distance from bead α of rod 1 to bead β of rod 2. κ is the inverse Debye screening length with

$$\kappa^2 = (\beta/\epsilon\epsilon_0)\sum_i \rho_i q_i^2 \tag{2}$$

Here ϵ is the dielectric constant of the solvent, $\beta = (k_B T)^{-1}$, $\sum_i \rho_i q_i^2$ denotes the sum over the densities of all kinds of small ions times their charges squared, and a is the hard-core radius of the beads.

The property of main interest is $g(\mathbf{r},\mathbf{u}_1,\mathbf{u}_2)$, the probability density of finding a rod with orientation given by the unit vector $\mathbf{u}_2$ and center of mass at $\mathbf{r}$, given another rod of orientation $\mathbf{u}_1$ with center of mass at the origin. This function is given by

$$g(\mathbf{r},\mathbf{u}_1,\mathbf{u}_2) = \frac{(4\pi V)^2 \int \mathrm{d}^2u_3\, \mathrm{d}^3r_3 \ldots \mathrm{d}^2u_N\, \mathrm{d}^3r_N \exp[-\beta \sum_{i<j} U(\mathbf{r}_{ij},\mathbf{u}_i,\mathbf{u}_j)]}{\int \mathrm{d}^2u_1\, \mathrm{d}^3r_1 \ldots \mathrm{d}^2u_N\, \mathrm{d}^3r_N \exp[-\beta \sum_{i<j} U(\mathbf{r}_{ij},\mathbf{u}_i,\mathbf{u}_j)]} \tag{3}$$

0024-9297/86/2219-1729$01.50/0

With the knowledge of $g(\mathbf{r},\mathbf{u}_1,\mathbf{u}_2)$ all averages in the phase space over two-particle functions can be calculated. On the other hand, we can define the averaged radial distribution function $\bar{g}(r)$ by integrating out the orientational degrees of freedom

$$\bar{g}(r) = \left(\frac{1}{4\pi}\right)^2 \int g(\mathbf{r},\mathbf{u}_1,\mathbf{u}_2)\, \mathrm{d}^2u_1\, \mathrm{d}^2u_2 \qquad (4)$$

The radial distribution function $g(\mathbf{r},\mathbf{u}_1,\mathbf{u}_2)$ and its average $\bar{g}(r)$ are, for example, important for determining the scattering intensity of the system. For *homogeneous* rods of length L in an isotropic solution the intensity of scattered radiation is proportion to[5]

$$I(k) = F(k) + \frac{\rho}{(4\pi)^2} \int \mathrm{d}^2u_1\, \mathrm{d}^2u_2\, \mathrm{d}^3r\, e^{i\mathbf{k}\cdot\mathbf{r}} j_0\left(\frac{L}{2}\mathbf{k}\cdot\mathbf{u}_1\right) \times j_0\left(\frac{L}{2}\mathbf{k}\cdot\mathbf{u}_2\right)(g(\mathbf{r},\mathbf{u}_1,\mathbf{u}_2) - 1) \qquad (5)$$

where $j_0(x) = \sin(x)/x$ and $F(k)$ is the form factor of one rod.[9] Equation 5 applies if $kd \ll 1$, where d is the diameter of the rods. Therefore, we are in a regime where the finite thickness of the rods can be neglected and $F(k)$ refers to infinitely thin rods. We define the static structure factor of the system by $S(k) = I(k)/F(k)$. Only for $kL \ll 1$ does $S(k)$ reduce to the simple result

$$S(k) = 1 + \rho \int \mathrm{d}^3r\, e^{i\mathbf{k}\cdot\mathbf{r}}(\bar{g}(r) - 1) \qquad (6)$$

which is identical with that for spherically symmetric particles.[10] For larger values of kL the averaged function $\bar{g}(r)$ is insufficient to calculate $S(k)$ and therefore $g(\mathbf{r},\mathbf{u}_1,\mathbf{u}_2)$ is needed. This also means that a measurement of $I(k)$ will give no information about $\bar{g}(r)$ and the mean center-to-center distance of the rods. In contrast to the case of spheres the static structure factor for rods depends on the shape of the particles.

The simulations were performed for a system of 256 dumbbells with the usual Monte Carlo technique[11] and periodic boundary conditions. The distance between the two beads of one dumbbell is kept fixed to the value $L/3^{1/2}$ for each run, respectively. At the beginning of the simulations all rods are aligned in the z direction and their centers of mass are fixed to a fcc lattice. After a thermalization of 30 000 Monte Carlo steps the next 400 configurations with a distance of 5000 steps were used to evaluate the averages. The system parameters were chosen as 0.0086 rod/(1000 Å)^3 for the concentration and Q = 150e. The dielectric constant of the solvent is e = 78.3 and the salt concentration was taken as 0.001 mol/m^3. The hard-core radius of the beads was 230 Å. To speed up the simulations, we cut off the potential of a given rod at a distance 0.28 L_k, where L_k = 30 952 Å is the length of one side of the simulation box. The interaction energy between the beads at this distance is 0.078kT. Simulations for spheres with a cutoff at 0.5L_k showed no differences.

Results of the Monte Carlo Simulations

The solid line in Figure 1 shows the radial distribution function $g_0(r)$ of a system of spheres (L = 0). The particular system parameters chosen above yield a main maximum of $g_0(r)$ at r_{max} about 5000 Å.

For $L \neq 0$ the distribution $g(\mathbf{r},\mathbf{u}_1,\mathbf{u}_2)$ as a function of the center of mass distance $\mathbf{r}$ will obviously depend on the relative orientations of the three vectors $\mathbf{r}$, $\mathbf{u}_1$, and $\mathbf{u}_2$. To illustrate that increasing influence, the following four configurations will be analyzed in greater detail.

(a) If $\mathbf{u}_1$, $\mathbf{u}_2$, and $\mathbf{r}$ are parallel to each other, the configuration is called the I configuration. Of all possible relative orientations this one has the highest interaction energy at a fixed distance.

(b) The T configuration is defined by $\mathbf{r}$ being parallel to one of the $\mathbf{u}$'s and perpendicular to the other one. Here, the energy is similar to the angle-averaged energy between the rods.

(c) If the rods are parallel to each other and perpendicular to $\mathbf{r}$, the configuration is denoted by H and the energy of this configuration is rather low.

(d) Finally, the lowest value of the energy is obtained in the X configuration, where $\mathbf{u}_1$, $\mathbf{u}_2$, and $\mathbf{r}$ are all perpendicular to each other.

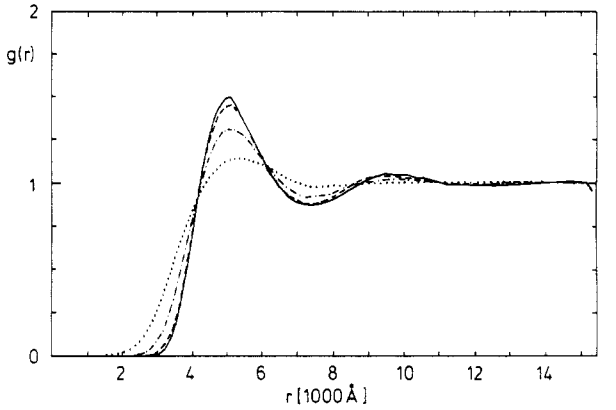

Figure 1. Averaged radial distribution function $\bar{g}(r)$ for L = 0 (spheres) (solid line), L/r_{max} = 0.64 (dashed line), L/r_{max} = 0.95 (dashed–dotted line), and L/r_{max} = 1.28 (dotted line).

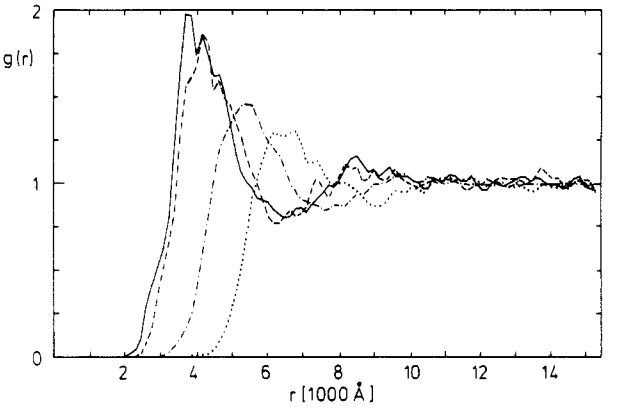

Figure 2. Radial distribution function for rods of length L = 0.95r_{max} for the X configuration (solid line), H configuration (dashed line), T configuration (dashed–dotted line), and I configuration (dotted line).

The distribution functions $g_i(r)$ with i = I, T, H, and X have been extracted from the simulations for various values of L/r_{max} up to 1.28. The results for L/r_{max} = 0.95 are shown in Figure 2. The splittings of the distribution functions for the different configurations increase with increasing length, since the difference in energy between the various configurations becomes larger.

Results for $\bar{g}(r)$, which averages according to eq 4 over *all* configurations, are displayed in Figure 1 for three values of $L > 0$ and are compared to $g_0(r)$. In contrast to $g_i(r)$, which exhibit strong short-range order, $\bar{g}(r)$ shows less structure with increasing L, since the correlations in the center-of-mass distances diminish as a result of the splittings in energy.

It is interesting to note that $\bar{g}(r)$ for the case $L = 0.64r_{max}$ is almost identical with $g_0(r)$, although clear splittings in the angle-dependent distribution functions exist already. This suggests an attempt to calculate the distribution functions by using an angle-averaged reference potential

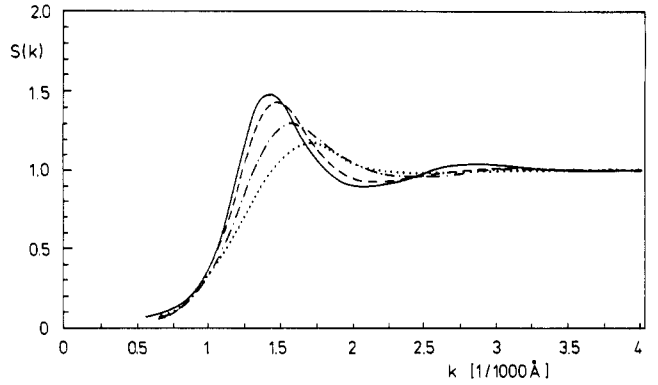

Figure 3. Structure factor $S(k)$ for $L = 0$ (spheres) (solid line), $L/r_{max} = 0.64$ (dashed line), $L/r_{max} = 0.95$ (dashed–dotted line), and $L/r_{max} = 1.28$ (dotted line).

plus an angle-dependent perturbation for L up to about 0.7. This procedure is well-known in the theory of molecular liquids,[12,13] where the reference potential is usually a hard-core or a Lennard-Jones potential and the perturbation is a dipole–dipole or a quadrupole–quadrupole interaction. Here, the reference potential would be chosen to be the monopole–monopole interaction. In contrast to the molecular liquid case, our perturbation will contain, among other terms, monopole–higher multipole interactions. This requires the knowledge of the three-particle distribution function in the reference system. Work to apply this perturbation theory is in progress.

As an application to a physical property which is experimentally accessible and which depends on the angle-dependent distribution function, we have calculated the structure factor $S(k)$. Details are given in the Appendix and the results are shown in Figure 3 for the same values of L as in Figure 1. Similar to $\bar{g}(r)$, the structure factor is seen to lose its peak with increasing length, but the most interesting property of $S(k)$ is the L dependence of k_{max}, which denotes the position of the peak of $S(k)$. Compared to the structure factor calculated form $\bar{g}(r)$ with (6), whose peak position is independent of L, the maximum of $S(k)$ is shifted to larger values of k.

Discussion of the Results

Charged rods in dilute solution are studied with Monte Carlo simulations. The interaction between different rods is modeled by the sum of the screened Coulomb interactions between two beads on each rod. The length and the charge of the dumbbells were determined by the requirement that the monopole and the quadrupole of both objects coincide. This model is expected to be reasonable for systems where the rod length is smaller than the mean distance between their centers of mass and where the shielding length $\varkappa^{-1}$ is comparable to or even larger than the rod length. Furthermore, we performed simulations with objects consisting of three segments (and a cutoff around 15 000 Å), and preliminary results are in good agreement with the results presented here.

The effect of the variation of the length of the rods on the distribution function, the averaged distribution function, and the static structure factor was studied in the low-density limit. The distribution function shows an increasing dependence on the orientations of the axes of the rods and the distance vector between them. This is due to the increasing influence of these orientations on the interaction energy between the rods. On the other hand, the averaged distribution function is seen to lose its structure with increasing length, without changing the position of its peak. The static structure factor is found to exhibit less structure but an increase of k_{max}, which denotes the position of its peak. This result shows that calculating $S(k)$ from the Fourier transform of $\bar{g}(r)$ is only useful for rather small values of L/r_{max}.

The position of the peak of the $\bar{g}(r)$ is independent of the rod length and therefore will show a concentration dependence as $c^{-1/3}$. However, k_{max} depends on the rod length, which indicates that the concentration dependence of k_{max} will scale with an exponent larger than 1/3 due to the additional L/r_{max} dependence of k_{max} in eq 5 as compared to eq 6. This might indicate an approach to the experimentally obtained $c^{1/2}$ behavior of k_{max} in the semidilute regime.[4]

Appendix

In this appendix we give some details about the calculation of the static structure factor $S(k)$ from the angle-dependent distribution function $g(\mathbf{r},\mathbf{u}_1,\mathbf{u}_2)$. From eq 5

$$S(k) = 1 + \frac{\rho}{(4\pi)^2 F(k)} \int d^2u_1\, d^2u_2\, d^3r\; h(\mathbf{r},\mathbf{u}_1,\mathbf{u}_2) e^{i\mathbf{k}\cdot\mathbf{r}} j_0\left(\frac{L}{2}\mathbf{k}\cdot\mathbf{u}_1\right) j_0\left(\frac{L}{2}\mathbf{k}\cdot\mathbf{u}_2\right) \quad \text{(A.1)}$$

where $h(\mathbf{r},\mathbf{u}_1,\mathbf{u}_2) = g(\mathbf{r},\mathbf{u}_1,\mathbf{u}_2) - 1$ is the total correlation function. Following a method used for molecular liquids[13] we expand $h(\mathbf{r},\mathbf{u}_1,\mathbf{u}_2)$ in a rotationally invariant form

$$h(\mathbf{r},\mathbf{u}_1,\mathbf{u}_2) = \sum_{l_1 l_2 l} h(l_1,l_2,l;r) \sum_{m_1 m_2 m} C(l_1,l_2,l;m_1,m_2,m) Y_{l_1 m_1}(\mathbf{u}_1) Y_{l_2 m_2}(\mathbf{u}_2) \times Y_{lm}^*(\hat{\mathbf{r}}) \quad \text{(A.2)}$$

where $Y_{l,m}(\mathbf{x})$ are spherical harmonics and $C(l_1,l_2,l;m_1,m_2,m)$ are Clebsch–Gordan coefficients.

The expansion coefficients in (A.2) are given by

$$h(l_1,l_2,l;r) = \frac{1}{C(l_1 l_2 l;000)} \int d^2u_1\, d^2u_2\, d^2\hat{r}\; h(\mathbf{r},\mathbf{u}_1,\mathbf{u}_2) Y_{l_1 0}(\mathbf{u}_1) Y_{l_2 0}(\mathbf{u}_2) Y_{l0}(\hat{\mathbf{r}}) \quad \text{(A.3)}$$

From the symmetry of the problem and the properties of the Clebsch–Gordan coefficients only even values of l_1, l_2, and l appear; furthermore, l is restricted to $|l_1 - l_2| \le l \le l_1 + l_2$ and $h(l_1,l_2,l) = h(l_2,l_1,l)$.

Taking $\mathbf{k}$ parallel to the z direction and using the Rayleigh expansion for $\exp(i\mathbf{k}\cdot\mathbf{r})$ and the expansion

$$j_0\left(\frac{L}{2}\mathbf{k}\cdot\mathbf{u}\right) = \sum_{l\ge 0} (4\pi)^{1/2} a_l(kL) Y_{l0}(\mathbf{u})$$

with

$$a_l(kL) = 0 \qquad \text{for } l = 1, 3, 5, \ldots \quad \text{(A.4a)}$$

$$a_l(kL) = i^l (2l+1)^{1/2} \frac{2}{kL} \int_0^{kL/2} j_l(x)\, dx \qquad \text{for } l = 0, 2, 4, \ldots \quad \text{(A.4b)}$$

and $j_l(x)$ denoting the lth spherical Bessel function, eq A.1 can be rewritten as

$$S(k) = 1 + \sum_{l_1 l_2 l} S_{l_1 l_2 l}(k) \quad \text{(A.5)}$$

where

$$S_{l_1 l_2 l}(k) = \frac{\rho/(4\pi)^{1/2}}{F(k)} i^l (2l+1)^{1/2} \times a_{l_1}(kL) a_{l_2}(kL) C(l_1,l_2,l;000) \int dr\, r^2 j_l(kr) h(l_1 l_2 l;r) \quad \text{(A.6)}$$

Using the coefficients $a_l(kL)$ the form factor of the rods can be expressed as

$$F(k) = \sum_l a_l^2(kL) \quad \text{(A.7)}$$

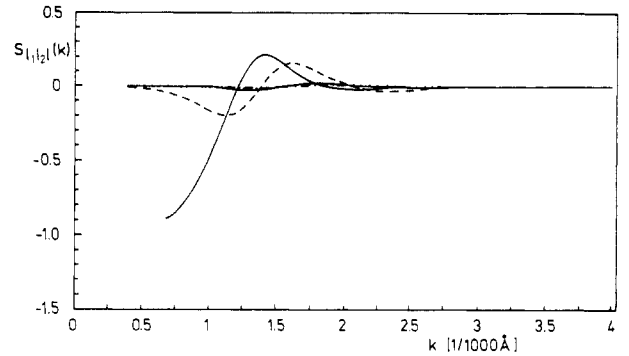

Figure 4. Components of $S(k)$ as defined in (A.6) for L/r_{max} = 0.95. $S_{000}(k)$ solid line), $S_{202} + S_{022}$ (dashed line), S_{220} (dashed-dotted line), S_{222} (dotted line), and S_{224} (solid line with $S_{224}(0) = 0$).

Of particular interest is the contribution of the term with $l = l_1 = l_2 = 0$ to $S(k)$, since it is related to the Fourier transform of the averaged distribution function $\bar{g}(r)$

$$S_{000}(k) = \frac{a_0^2(kL)}{F(k)} \rho \int d^3r \, e^{i\mathbf{k}\cdot\mathbf{r}}(\bar{g}(r) - 1) \qquad (A.8)$$

For small L with $kL < 1$, all $a_l(kL)$ for $l > 0$ are much smaller than $a_0(kL)$. In this case, the sum in (A.5) can be well approximated by its first term (A.8), and by using (A.7) for the form factor, (A.5) reduces to eq 6.

If $kL < 10$, it is sufficient to consider a_0 and a_2 only, since all other a_l are still small. In this case, the structure factor is approximately given by

$$S(k) = 1 + S_{000}(k) + 2S_{202}(k) + S_{220}(k) + S_{222}(k) + S_{224}(k) \qquad (A.9)$$

$S_{202}(k)$ is counted twice, since $S_{022} = S_{202}$. The components used in (A.9) to calculate $S(k)$ are shown in Figure 4 for $L/r_{max} = 0.95$. For all values of L considered, $k_{max}L$ is smaller than 10 and the components S_{220}, S_{222}, and S_{224} are found to be small. Therefore (A.9) is sufficient to calculate $S(k)$ for these values of L/r_{max}.

References and Notes

(1) Hansen, J. P.; Hayter, J. B. *Mol. Phys.* **1982**, *46*, 651. Hayter, J. B.; Penfold, J. *Mol. Phys.* **1981**, *42*, 109.
(2) van Megen, W.; Snook, J. *J. Chem. Phys.* **1977**, *66*, 813.
(3) Hoffmann, H.; Kalus, J.; Thurn, H.; Ibel, K. *Ber. Bunsenges. Phys. Chem.* **1983**, *87*, 1120.
(4) Drifford, M.; Dalbiez, J. P. *J. Phys. Chem.* **1984**, *88*, 5368.
(5) Schneider, J.; Hess, W.; Klein, R. *J. Phys. A* **1985**, *18*, 1221.
(6) Benmouna, M.; Weill, G.; Renoit, H.; Akcasu, A. Z. *J. Phys. (Paris)* **1982**, *43*, 1679.
(7) Brenner, S. L.; Parsegian, V. A. *Biophys. J.* **1974**, *14*, 327.
(8) For the application to scattering experiments on growing micelles one has to take into account that the rodlike micelles contain more monomers than spherical ones and therefore the total charge increases with L.
(9) Pecora, R. *J. Chem. Phys.* **1968**, *48*, 4126.
(10) Hansen, J. P.; McDonald, I. R. *Theory of Simple Liquids*; Academic: New York, 1976.
(11) Metropolis, N.; Rosenbluth, A. W.; Rosenbluth, M. N.; Teller, A. H.; Teller, E. *J. Chem. Phys.* **1953**, *21*, 1087.
(12) Street, W. B.; Gubbins, K. E. *Annu. Rev. Phys. Chem.* **1977**, *28*, 373.
(13) Gray, C. G.; Gubbins, K. E. *Theory of Molecular Fluids*; Clarendon: Oxford, 1984.

Analysis of Enthalpy Relaxation in Poly(methyl methacrylate): Effects of Tacticity, Deuteration, and Thermal History

John J. Tribone,* J. M. O'Reilly, and Jehuda Greener

Research Laboratories, Eastman Kodak Company, Rochester, New York 14650.
Received August 19, 1985; Revised Manuscript Received February 21, 1986

ABSTRACT: Precise differential scanning calorimetry measurements were used to assess the enthalpy relaxation behavior of hydrogenous and deuterated poly(methyl methacrylate) (PMMA), in each of the three stereospecific forms. These polymers provide a set of well-characterized materials with a systematic variation in structure with which the multiorder parameter model can be tested. Materials are held for various times at several sub-T_g annealing temperatures, and results are analyzed in the context of the multiorder parameter model of Narayanaswamy, Kovacs, Moynihan, et al., which assumes thermorheological simplicity, a distribution of relaxation times, and structure-dependent relaxation times. Deuteration has little or no effect on the relaxation behavior and tacticity manifests itself mainly in the magnitude of the activation energy, which scales with the glass transition temperature. The apparent activation energy and the parameter used to characterize the distribution of relaxation times are independent of annealing time and annealing temperature. However, the parameter that characterizes the structure dependence of the relaxation times systematically changes with thermal history, which contradicts its original introduction into the model as a material constant. In addition, the discrepancy between experiment and theory suggests that the model becomes less appropriate as the system approaches closer to equilibrium. It is suggested that the model may be improved by changing the form of the relaxation function and/or modifying the simplified way in which the structure dependence of the relaxation times is introduced.

I. Introduction

Over the years there has been a growing interest in the structural relaxation and recovery processes observed in glassy materials of all kinds, including molecular (organic),[1,2,5] inorganic,[3-5] polymeric,[1,2,6-19] and, more recently, metallic glasses.[20-22] The nature of the problem is clearly related to the intrinsic properties of the "ill-condensed", i.e., nonequilibrium, glassy state, as each of the above classes of materials shows remarkably similar structural relaxation behavior despite obvious differences in the chemical moieties and in the nature of the molecular or atomic forces involved.

Structural relaxation is a result of the nonequilibrium nature of the glassy state, which spontaneously evolves toward some equilibrium state (defined by T and P) at a rate that depends on the temperature, the pressure, and

0024-9297/86/2219-1732$01.50/0